Supplement of Atmos. Meas. Tech., 15, 2993–3009, 2022
https://doi.org/10.5194/amt-15-2993-2022-supplement

Atmospheric Measurement Techniques
Open Access
EGU

Supplement of

Intercomparison of holographic imaging and single-particle forward light scattering in situ measurements of liquid clouds in changing atmospheric conditions

Petri Tiitta et al.

Correspondence to: Petri Tiitta (petri.tiitta@fmi.fi)

Supplement S1: Cloud boundaries for LWC estimations

Condensation of water vapor introduces strong vertical variations of cloud properties that can be used to define cloud boundaries. However, the location of cloud boundaries depends on the variable and methodology selected to quantify these changes. For example, Mellado et al. (2017) defined cloud boundary as the cloudy-air/clear-air interface where liquid water content at the Kolmogorov scale (ca. 10 mm) increases from zero to mean in-cloud values.

From the modeling point of view, this definition is inconvenient because it is difficult to achieve such fine resolution with large-eddy simulations. A more feasible approach links cloudy conditions to grid points of the model domain where the liquid water content is equal to or above 0.01 g m^{-3} (Stevens et al., 2015) or 0.01 g kg^{-1} (Igel et al., 2017). From the experimental point of view, cloud boundaries are linked to variations in the vertical profiles of backscatter light obtained with in-situ or satellite remote sensing instruments (e.g. ceilometer, cloud radar, microwave radiometer). Threshold values in the signal strength versus height (i.e. radar reflectivity dBZ) are correlated to the presence of droplets, as droplets interfere with the free transmission of radiation through the atmosphere. The cloud radar signal is sensitive to the sixth power of droplet diameter and therefore, the cloud radar response is dominated by the largest droplets in the observation volume (Bühl et al., 2015).

Drastic changes in the vertical profile of radar reflectivity are expected to occur at the cloud top in liquid clouds where droplets are larger. Liu et al. (2008) studied the dependence between threshold reflectivity and droplet number concentration and summarized criteria used to distinguish between precipitating and nonprecipitating clouds (e.g., a jump of 10 dBZ in reflectivity to distinguish between drizzle-free and drizzle-containing clouds). In this study, experimental cloud base values were taken from the ceilometer and the doppler lidar, and cloud top height values were retrieved from profiles of radar reflectivity dBz measured with the millimeter-wave cloud radar, all instruments at the Savilahti measurement station (Finnish Meteorological Institute: Observations at Kuopio Savilahti station). Radars are located at the building roof c.a. 87 m above ground level, therefore the Doppler lidar can perform direct line-of-sight scanning above the Puijo tower (Hirsikko et al., 2014). Cloud top height values were retrieved from 3 s time series of the radar reflectivity vertical profile. They were numerically linked to the maximum altitude at which there was a continuous dBZ signal in the vertical direction followed by signal absence at the consecutive higher atmospheric layer. The quality of retrieved values was qualitatively assessed by overlapping them with cloud radar profiles. Retrieved cloud top values corresponded to reflectivity ranging between -20 dBZ and -30 dBZ, typical values for haze droplets.

References

Bühl, J., Leinweber, R., Görsdorf, U., Radenz, M., Ansmann, A., and Lehmann, V.: Combined vertical-velocity observations with Doppler lidar, cloud radar and wind profiler, Atmos. Meas. Tech., 8, 3527–3536, https://doi.org/10.5194/amt-8-3527-2015, 2015.

Finnish Meteorological Institute: Observations at Kuopio Savilahti station, https://hav.fmi.fi/hav/asema/index.php?fmisid=101586&page=obs&begdate=24.09.2020&enddate=24.09.2020&dataset=fmisid_instant_1min&TA=on

Hirsikko, A., O'Connor, E. J., Komppula, M., Korhonen, K., Pfüller, A., Giannakaki, E., Wood, C. R., Bauer-Pfundstein, M., Poikonen, A., Karppinen, T., Lonka, H., Kurri, M., Heinonen, J., Moisseev, D., Asmi, E.,

Aaltonen, V., Nordbo, A., Rodriguez, E., Lihavainen, H., Laaksonen, A., Lehtinen, K. E. J., Laurila, T., Petäjä, T., Kulmala, M., and Viisanen, Y.: Observing wind, aerosol particles, cloud and precipitation: Finland's new ground-based remote-sensing network, Atmos. Meas. Tech., 7, 1351–1375, https://doi.org/10.5194/amt-7-1351-2014, 2014.

Igel, A. L. and van den Heever, S. C.: The importance of the shape of cloud droplet size distributions in shallow cumulus clouds. Part II: Bulk microphysics simulations, J. Atmos. Sci., 74, 259–273, https://doi.org/10.1175/JAS-D-15-0383.1, 2017.

Liu, Y., Geerts, B., Miller, M., Daum, P., and McGraw, R.: Threshold radar reflectivity for drizzling clouds, Geophys. Res. Lett., 35, L03807, https://doi.org/10.1029/2007GL031201, 2008.

Mellado, J. P. Cloud-top entrainment in stratocumulus clouds, Annual Review of Fluid Mechanics, 49, 145–169, https://doi. org/10.1146/annurev-fluid-010816-060231, 2017.

Stevens, B., Moeng, C. H., Ackerman, A. S., Bretherton, C. S., Chlond, A., de Roode, S., Edwards, J., Golaz, J. C., Jiang, H., Khairoutdinov, M., Kirkpatrick, M. P., Lewellen, D. C., Lock, A., Müller, F., Stevens, D. E., Whelan, E., & Zhu, P.: Evaluation of large-eddy simulations via observations of nocturnal marine stratocumulus, Monthly Weather Review, 133(6), 1443– 1462, https://doi.org/10.1175/MWR2930.1, 2005.

Supplement S2: Probability distributions for MC analyses

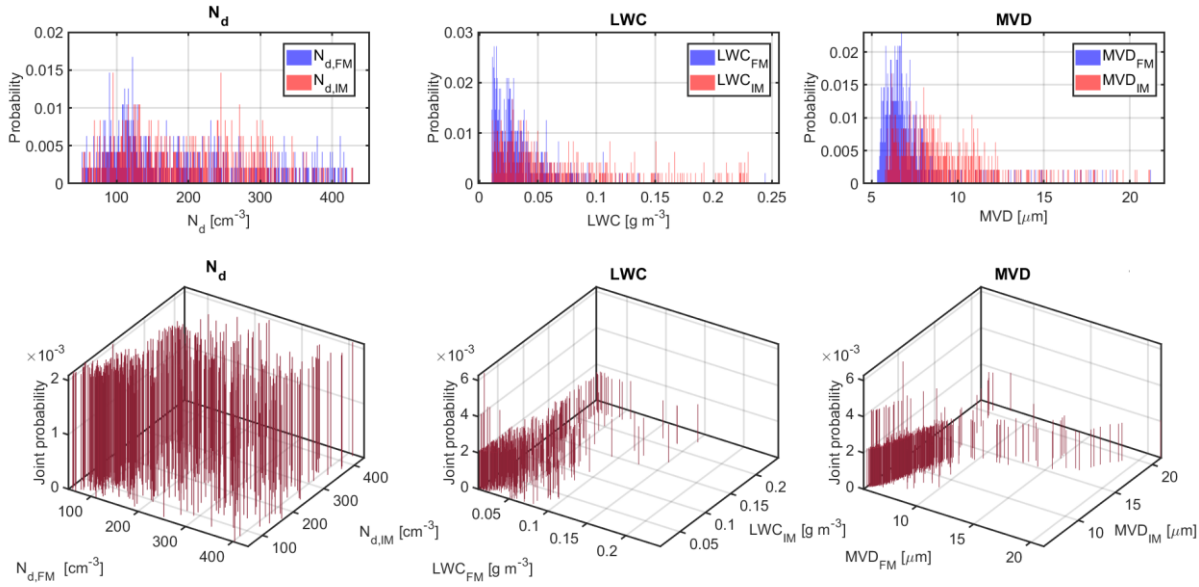

Figure S1: Probability and Joint Probability distributions for observations of the FM-120 and the ICEMET instruments.

In the upper plots in Figure S1 we can notice the degree of overlapping between probability distributions of our compared variables along with the measurement range. Joint histograms in the lower plots are just the commonalities between data sets. While the degree of shared information for droplet number concentrations is high in general for all the variable ranges, the information shared between distributions of liquid water content and median volume diameter decreases when increasing magnitude for these variables. Since LWC and MVD are connected to the third power of the droplet diameter, the sparseness of data points in these areas suggests an increment in measurement uncertainties when droplet sizes are larger or approaching the upper size detected by the fog monitor (~ 50 μm). It is also likely that the algorithms used for estimations of median volume diameter fail in two specific situations when there are few very large droplets mixed with smaller ones and the mass distribution is bimodal (Figure S2), or when large number concentrations of small droplets when 50% of the total mass is below the lower size detected by the instrument (Figure S3).

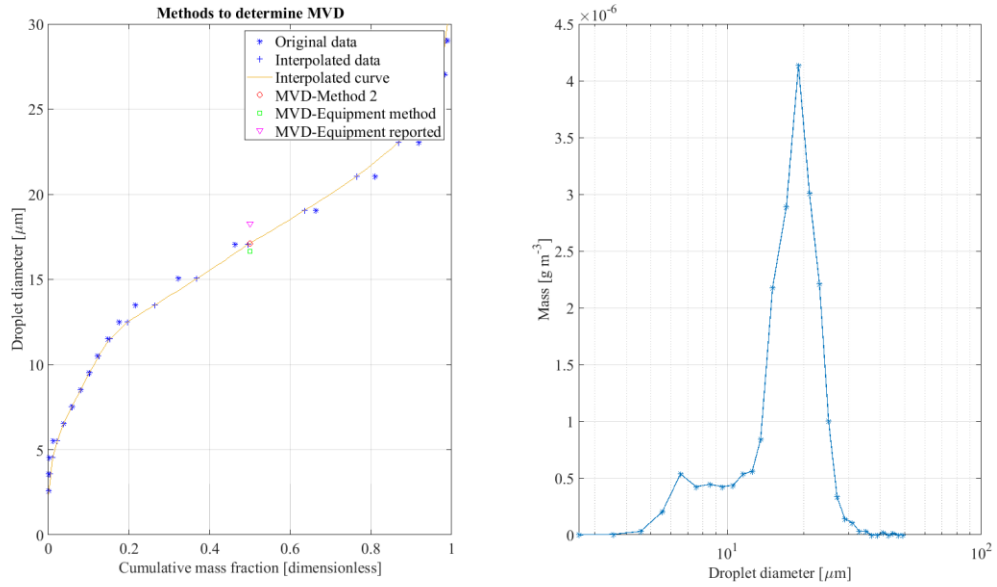

Figure S2: The estimation of the median volume diameter when the mass size distribution is bimodal.

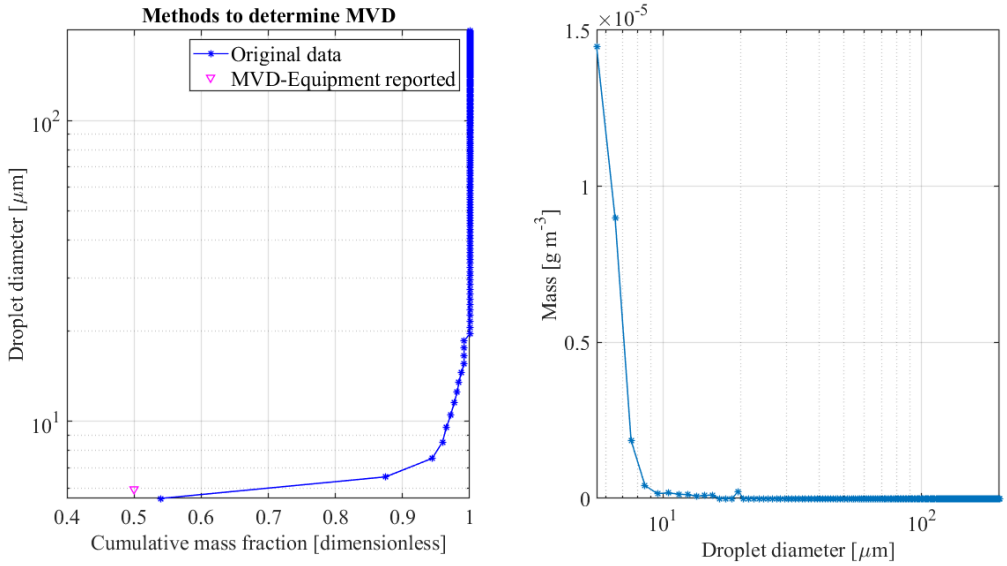

Figure S3: The estimation of the median volume diameter when the total mass is dominated by droplets with size below the minimal size detected by the equipment.